Structure and Bonding in First-Row Transition Metal Dicarbide Cations MC_2^+

Víctor M. Rayón,* Pilar Redondo, Carmen Barrientos, and Antonio Largo*

Departamento de Química Física y Química Inorgánica, Facultad de Ciencias, Universidad de Valladolid, 47005 Valladolid, Spain

Received: November 29, 2006; In Final Form: March 6, 2007

A theoretical study of the first-row transition metal dicarbide cations MC_2^+ (M = Sc−Zn) has been carried out. Predictions for different molecular properties that could help in their eventual experimental detection have been made. Most MC_2^+ compounds prefer a C_{2v} symmetric arrangement over the linear geometry. In particular, the C_{2v} isomer is specially favored for early transition metals. Only for CuC_2^+ is the linear isomer predicted to be the global minimum, although by only 1 kcal/mol. In all cases the isomerization barrier between cyclic and linear species seems to be very small (below 2 kcal/mol). The topological analysis of the electronic density shows that most C_{2v} isomers are T-shaped structures. In general, MC_2^+ compounds for early transition metals have larger dissociation energies than those formed by late transition metals. In most cases the dissociation energies for MC_2^+ compounds are much smaller than those obtained for their neutral analogues. An analysis of the bonding in MC_2^+ compounds in terms of the interactions between the valence orbitals of the fragments helps to interpret their main features.

Introduction

Binary compounds between transition metals and carbon atoms have received much attention in recent years, mainly due to their relevance as building blocks of a variety of new materials with potential important applications. For instance, early transition metals form stable metal−carbon clusters with M_8C_{12} stoichiometry known as metallocarbohedrenes[1−6] (met-cars for short). The corresponding ions, such as $Ti_8C_{12}^+$, have also been studied by infrared spectroscopy.[7] Experimental[8,9] and theoretical studies[10−13] on met-cars suggest that the most likely structure is a tetracapped tetrahedron with T_d symmetry,[6] whose basic structural subunit seems to be MC_2, since the metal is bonded to C_2 units. Transition metals can also be incorporated into carbon clusters to form networked metallofullerenes.[14] On the other hand, rare-earth elements can be trapped inside fullerene cages to form endohedral metallofullerenes.[15] Finally, late transition metals are catalysts for carbon nanotube formation.[16] It seems that to a great extent the type of structure formed is dictated by the nature of the interaction between the transition metal and carbon. It is therefore important to have a detailed knowledge of the interaction in binary metal−carbon compounds that can be the building blocks for these new materials, and for this purpose theoretical studies can be very helpful.

Obviously, metal dicarbides are quite interesting subjects in this context, as possible building blocks and also as the smallest kind of binary carbides where a competition between different isomers (cyclic and linear) can be found. Some theoretical studies have been conducted on MC_2 molecules, most of them dealing with a single compound.[17−30] A more general study for MC_2 compounds (M = Sc, V, Cr, Mn, Fe, and Co), based on the results from photoelectron spectra, has been carried out by Li and Wang.[31] In addition, we have recently contributed with a theoretical systematic study of MC_2 compounds across the first-row transition series (M = Sc−Zn).[32] Even more scarce is the available information on charged metal dicarbides, even though MC_2^+ species are potential interesting targets for experimental studies by infrared spectroscopy.[7] For example, a recent theoretical prediction of the structure and IR spectrum of TiC_2^+ has been reported.[33]

In this paper we report a systematic study of MC_2^+ (M = Sc−Zn) cations. We will provide structural information that could be helpful to guide experimental search of these species, as well as a detailed study of the bonding in these compounds in order to identify the nature of the interactions, which is essential to understand their stability.

Computational Methods

The theoretical methods employed in this work are identical to those used in the study of their neutral counterparts.[32] Therefore, two different theoretical approaches have been applied for obtaining geometrical parameters. Density functional theory (DFT) calculations, with the B3LYP exchange-correlation functional,[34,35] have been carried out in order to optimize the geometry. This functional includes the Lee−Yang−Parr[36] correlation functional in conjunction with a hybrid exchange functional first proposed by Becke.[37] It has been shown in previous studies that such an approach provides good agreement with the experimental results in medium-sized heteroatom-doped carbon clusters.[38] Additional geometry optimizations have been performed at the QCISD level.[39] This stands for quadratic configuration interaction including single and double excitations. In both cases, B3LYP and QCISD, we employed different basis sets, but we will only report those results obtained with the basis set denoted as 6-311+G(3df). This basis set includes diffuse and polarization functions and is constructed by employing the triple split-valence 6-311G[40] for carbon atoms, and the Wachters[41] and Hay[42] basis set with the scaling factor of Ragavachari and Trucks[43] for the first-row transition metal. Harmonic vibrational calculations have been performed at the B3LYP level with the 6-311+G(3df) basis set. In the case of the QCISD method, the 6-311+G(d) basis set was employed [at the

* Authors to whom correspondence should be addressed: fax 34-983-423013; e-mail vmrr@qf.uva.es (V.M.R.) or alargo@qf.uva.es (A.L.).

10.1021/jp0679055 CCC: $37.00
Published on Web 06/20/2007

TABLE 1: Electronic Configurations, Geometrical Parameters, and Harmonic Vibrational Frequencies for Linear MC_2^+ Species[a]

		linear geometry		
linear MC_2^+	electronic configuration	R(X−C), Å	R(C−C), Å	vibrational frequencies (cm^{-1})
ScC_2^+ ($^1\Sigma^+$)[b]	{core}$8\sigma^2 9\sigma^2 3\pi^4 10\sigma^2$	1.840 (1.882)	1.297 (1.319)	106i(π), 646(σ), 1800(σ)
		1.846	1.303	60i(π), 647(σ), 1751(σ)
TiC_2^+ ($^2\Delta$)	{core}$8\sigma^2 9\sigma^2 3\pi^4 10\sigma^2 1\delta^1$	1.798 (1.858)	1.303 (1.332)	56i(π), 624(σ), 1776(σ)
		1.861	1.314	81(π), 391(σ), 1719(σ)
VC_2^+ ($^5\Delta$)	{core}$8\sigma^2 9\sigma^2 3\pi^4 10\sigma^1 1\delta^1 4\pi^2$	1.970 (2.031)	1.235 (1.248)	154(π), 516(σ), 1926(σ)
		1.929	1.229	48(π), 527(σ), 1954(σ)
CrC_2^+ ($^6\Sigma^+$)	{core}$8\sigma^2 9\sigma^2 3\pi^4 10\sigma^1 1\delta^2 4\pi^2$	1.918 (1.981)	1.233 (1.246)	171(π), 538(σ), 1941(σ)
		1.890	1.227	176(π), 543(σ), 1975(σ)
MnC_2^+ ($^7\Sigma^+$)	{core}$8\sigma^2 9\sigma^2 3\pi^4 10\sigma^1 1\delta^2 4\pi^2 11\sigma^1$	1.890 (2.013)	1.229 (1.234)	167(π), 530(σ), 1970(σ)
		1.934	1.231	155(π), 516(σ), 1959(σ)
FeC_2^+ ($^6\Delta$)	{core}$8\sigma^2 9\sigma^2 3\pi^4 10\sigma^1 1\delta^3 4\pi^2 11\sigma^1$	1.848 (1.947)	1.232 (1.246)	176(π), 547(σ), 1949(σ)
		1.873	1.234	176(π), 546(σ), 1917(σ)
CoC_2^+ ($^5\Pi$)[c]	{core}$8\sigma^2 9\sigma^2 3\pi^4 10\sigma^2 1\delta^2 4\pi^3 11\sigma^1$	1.836 (1.928)	1.236 (1.243)	242i(π), 227(π), 521(σ), 1951(σ)
		1.842	1.232	179(π), 207(π), 552(σ), 1956(σ)
NiC_2^+ ($^4\Sigma^-$)	{core}$8\sigma^2 9\sigma^2 3\pi^4 10\sigma^2 1\delta^4 4\pi^2 11\sigma^1$	1.791 (1.903)	1.258 (1.245)	382(π), 539(σ), 1755(σ)
		1.813	1.276	567i(π), 491(σ), 1688(σ)
CuC_2^+ ($^3\Pi$)[c]	{core}$8\sigma^2 9\sigma^2 3\pi^4 10\sigma^2 1\delta^4 4\pi^3 11\sigma^1$	1.852 (2.009)	1.269 (1.289)	90(π), 260(π), 438(σ), 1829(σ)
		1.865	1.274	197(π), 278(π), 450(σ), 1852(σ)
ZnC_2^+ ($^2\Sigma^+$)	{core}$8\sigma^2 9\sigma^2 3\pi^4 10\sigma^2 1\delta^4 4\pi^4 11\sigma^1$	1.839 (1.867)	1.210 (1.237)	73i(π), 543(σ), 2130(σ)
		1.839	1.219	123(π), 553(σ), 2075(σ)

[a] Obtained with the B3LYP/6-311+G(3df), QCISD/6-311+G(3df) (second line), and CASSCF/6-311+G(d) (in parentheses) methods. QCISD vibrational frequencies have been computed with the 6-311+G(d) basis set. [b] QCISD values obtained with the LAN/-6+(d) basis set (see text for description). [c] Note that nondegenerate π vibrational frequencies, corresponding to the two Renner−Teller components, are obtained in this case.

corresponding QCISD/6-311+G(d) geometries]. Zero-point vibrational energies (ZPVE) were computed by employing the harmonic vibrational frequencies.

Single-point calculations at the CCSD(T) level[44] (coupled-cluster single and double excitation model augmented with a noniterative treatment of triple excitations) employing the 6-311+G(3df) basis set have been carried out on the QCISD/6-311+G(3df) geometries in order to refine the electronic energy. In all correlated calculations we have included the valence electrons of the carbon atoms and the 4s and 3d electrons of the metal. The atomic states have been obtained following the rules given by Hay[42] for occupation of the d orbitals. All these calculations were carried out with the Gaussian-98 program package.[45]

In order to take into account the possible multiconfigurational nature of the compounds under study, we have carried out CASSCF (complete active space multiconfiguration self-consistent field) optimizations followed by MRCI (multireference singles and doubles configuration interaction) single-point calculations to improve the energy. In these multiconfigurational calculations we employed the 6-311+G(d) basis set. The reference CAS space was constructed by distributing all valence electrons in 13 orbitals (including the 4s and 3d orbitals of the metal and four occupied and three unoccupied orbitals of the dicarbide moiety). For the MRCI calculations, the valence electrons of the carbon atoms and the 4s and 3d electrons of the metal have been correlated. This is a relatively large number of active electrons that makes the MRCI calculations extremely computationally demanding. We have therefore not used the full CASSCF wavefunction as reference. Instead, we have chosen those configurations with a coefficient larger than a certain value, in all cases within the range 0.01−0.05. In order to compute reliable relative energies of cyclic and linear isomers, we have checked that the weight of the selected configurations for a given transition metal is about the same in both conformations. The MOLPRO suite of programs[46] was employed for these calculations.

As in our previous study on MC_2 compounds,[32] we have not included relativity in our calculations for the systematic study of first-row transition metal dicarbide cations. Nevertheless, we have checked for the first (Sc) and last member of the series (Zn) that the influence of relativity corrections on the main geometrical and energetic properties is marginal.

The nature of bonding for the different MC_2 species was characterized through topological analysis of the electronic density.[47] These calculations were performed with the MORPHY program,[48] employing the QCISD/6-311+G(d) electronic density. An analysis in terms of natural bond orbitals (NBO)[49] has also been carried out.

Results and Discussion

Molecular Structure of MC_2^+ Cations. As in the case of their neutral parent molecules, dicarbide cations have M−C−C or M−C_2 connectivities. The isomers with the metal in central position, C−M−C, were found to lie much higher in energy. Different spin multiplicities were checked for each system, but results will be provided only for the lowest-lying spin state in each case.

The optimized geometries and harmonic (unscaled) vibrational frequencies for the linear and cyclic MC_2^+ isomers are given in Tables 1 and 2 , respectively. We should point out that in the case of linear ScC_2^+ ($^1\Sigma^+$) the QCISD optimizations with 6-311+G(d) and 6-311+G(3df) basis sets failed. Therefore, the QCISD geometrical parameters have been obtained in that case with the LAN-6+(d) basis set. This basis set employs the 6-311+G(d) basis set for carbon atoms and the LanL2DZ[50−52] for the transition metal, which includes an effective core potential treatment.

By comparison of Tables 1 and 2, it is readily noticed that the spin multiplicities of the lowest-lying linear and cyclic MC_2^+ species are different for VC_2^+, CrC_2^+, and MnC_2^+. We obtained optimized structures for VC_2^+ ($^3\Sigma^-$; ... $8\sigma^2 9\sigma^2 3\pi^4 10\sigma^2 1\delta^2$), CrC_2^+ ($^4\Sigma^-$; ... $8\sigma^2 9\sigma^2 3\pi^4 10\sigma^2 1\delta^2 11\sigma^1$), and MnC_2^+ ($^5\Sigma^+$; ... $8\sigma^2 9\sigma^2 3\pi^4 10\sigma^2 1\delta^2 4\pi^2$), which correlate with the corresponding lowest-lying cyclic species, but all of them lie higher in energy than their respective high-spin linear states shown in Table 1. In addition, the linear electronic state correlating with the lowest-

TABLE 2: Electronic Configurations, Geometrical Parameters, and Harmonic Vibrational Frequencies for Cyclic MC_2^+ Species[a]

		cyclic geometry			
cyclic MC_2^+	electronic configuration	R(X−C), Å	R(C−C), Å	−CXC, deg	vibrational frequencies (cm^{-1})
ScC_2^+ ($^1A_1$)	{core}$7a_1^2 4b_2^2 8a_1^2 3b_1^2 9a_1^2$	2.007 (2.022)	1.270 (1.294)	36.9 (37.3)	473(b_2), 684(a_1), 1794(a_1)
		1.981	1.265	37.3	454(b_2), 735(a_1), 1805(a_1)
TiC_2^+ ($^2A_2$)	{core}$7a_1^2 4b_2^2 8a_1^2 3b_1^2 9a_1^2 1a_2^1$	1.920 (1.992)	1.270 (1.301)	38.6 (38.1)	473(b_2), 720(a_1), 1777(a_1)
		1.956	1.274	38.0	458(b_2), 573(a_1), 1780(a_1)
VC_2^+ ($^3B_1$)	{core}$7a_1^2 4b_2^2 8a_1^2 3b_1^2 9a_1^2 5b_2^1 1a_2^1$	1.865 (1.926)	1.304 (1.311)	40.9 (39.8)	197(b_2), 854(a_1), 1653(a_1)
		1.850	1.310	41.5	420(b_2), 641(a_1), 1599(a_1)
CrC_2^+ ($^4B_1$)	{core}$7a_1^2 4b_2^2 3b_1^2 8a_1^2 9a_1^2 5b_2^1 1a_2^1 10a_1^1$	2.009 (2.008)	1.297 (1.305)	37.6 (37.9)	366(b_2), 402(a_1), 1664(a_1)
		1.966	1.300	38.6	354(b_2), 402(a_1), 1640(a_1)
MnC_2^+ ($^5A_1$)	{core}$7a_1^2 4b_2^2 3b_1^2 8a_1^2 9a_1^2 5b_2^1 1a_2^1 4b_1^1 10a_1^1$	2.064 (2.171)	1.274 (1.284)	36.0 (34.4)	199(b_2), 465(a_1), 1776(a_1)
		2.106	1.280	35.4	264(b_2), 473(a_1), 1747(a_1)
FeC_2^+ ($^6A_1$)	{core}$7a_1^2 4b_2^2 3b_1^2 8a_1^2 9a_1^2 5b_2^1 1a_2^1 4b_1^1 10a_1^1 11a_1^1$	1.987 (2.127)	1.276 (1.279)	37.5 (35.0)	347(b_2), 434(a_1), 1724(a_1)
		2.023	1.278	36.8	326(b_2), 506(a_1), 1748(a_1)
CoC_2^+ ($^5A_2$)	{core}$7a_1^2 4b_2^2 3b_1^2 8a_1^2 9a_1^2 5b_2^1 1a_2^2 4b_1^1 10a_1^1 11a_1^1$	1.932 (2.053)	1.284 (1.285)	38.8 (36.5)	390(b_2), 491(a_1), 1683(a_1)
		1.949	1.284	38.5	387(b_2), 479(a_1), 1712(a_1)
NiC_2^+ ($^4A_2$)	{core}$7a_1^2 4b_2^2 3b_1^2 8a_1^2 9a_1^2 5b_2^1 1a_2^2 4b_1^1 10a_1^2 11a_1^1$	1.928 (2.052)	1.282 (1.284)	38.8 (36.5)	376(b_2), 498(a_1), 1665(a_1)
		1.916	1.282	39.1	396(b_2), 521(a_1), 1713(a_1)
CuC_2^+ ($^3B_1$)	{core}$7a_1^2 4b_2^2 3b_1^2 8a_1^2 9a_1^2 5b_2^2 1a_2^2 4b_1^1 10a_1^2 11a_1^1$	2.001 (2.381)	1.324 (1.328)	38.6 (32.4)	222(b_2), 406(a_1), 1558(a_1)
		1.998	1.331	38.9	280(b_2), 466(a_1), 1553(a_1)
ZnC_2^+ ($^2A_1$)	{core}$7a_1^2 4b_2^2 3b_1^2 8a_1^2 9a_1^2 5b_2^2 1a_2^2 4b_1^1 10a_1^2 11a_1^1$	2.031 (2.084)	1.283 (1.289)	36.8 (36.0)	245(b_2), 472(a_1), 1736(a_1)
		2.017	1.288	37.2	253(b_2), 494(a_1), 1706(a_1)

[a] Obtained with the B3LYP/6-311+G(3df), QCISD/6-311+G(3df) (second line), and CASSCF/6-311+G(d) (in parentheses) methods. QCISD vibrational frequencies have been computed with the 6-311+G(d) basis set.

TABLE 3: NBO Atomic Charges at the QCISD/6-311+G(d) Level

atomic charge	Sc	Ti	V	Cr	Mn	Fe	Co	Ni	Cu	Zn
					Linear Isomer					
Q(M)	1.890	1.525	1.676	1.582	1.694	1.559	1.394	0.997	1.065	1.614
$Q(C_1)$	−1.161	−0.925	−0.980	−0.906	−1.036	−0.957	−0.621	−0.491	−0.482	−1.008
$Q(C_2)$	0.271	0.400	0.304	0.324	0.342	0.398	0.227	0.494	0.417	0.394
					Cyclic Isomer					
Q(M)	1.826	1.568	1.504	1.490	1.658	1.550	1.436	1.258	1.168	1.560
Q(C)	−0.413	−0.284	−0.252	−0.245	−0.329	−0.275	−0.218	−0.129	−0.084	−0.280

lying cyclic state for CoC_2^+, namely, $^5\Delta$ (... $8\sigma^2 9\sigma^2 3\pi^4 10\sigma^2 1\delta^3 4\pi^2 11\sigma^1$), also lies higher in energy than the $^5\Pi$ state.

In general, there is a reasonable agreement between the B3LYP and QCISD bond distances. The worst case is the M−C distance in linear TiC_2^+, where a difference of 0.063 Å is observed. On the other hand, CASSCF geometries show larger metal−ligand bond distances than B3LYP and QCISD geometries. The difference is, however, within 0.1 Å, which we consider to be reasonable when it is taken into account that CASSCF geometries do not include dynamic electron correlation besides that recovered in the MCSCF treatment. The exceptions are cyclic TiC_2^+ ($^2A_2$), FeC_2^+ ($^6A_1$), NiC_2^+ ($^4A_2$), and CuC_2^+ ($^3B_1$). Since these systems do not have large multireference character (see Table S3 in the Supporting Information) we think these larger differences are due to particularly strong dynamical correlation effects. Most C−C distances for linear isomers are quite similar and very close to the C−C distance in C_2 (1.247, 1.250, and 1.254 Å, respectively, at the B3LYP, QCISD, and CASSCF levels). The only exceptions are found for the two first members of the series, linear ScC_2^+ and TiC_2^+, with C−C distances that are larger than those found for their corresponding cyclic isomers. All C−C distances for cyclic MC_2^+ isomers are within the range 1.27−1.33 Å, beginning close to the C−C distance in C_2 and growing up to 1.33 Å for Cu.

The agreement between B3LYP and QCISD vibrational frequencies is also reasonably good. However, there are some qualitative discrepancies for linear isomers. Both levels of theory agree in that linear ScC_2^+ is in fact a transition state for the degenerate rearrangement of the corresponding cyclic isomer (because it has an imaginary vibrational frequency). However, in four cases (Ti, Co, Ni, and Zn) the nature of the linear isomer at both levels is opposite, with one imaginary frequency only at one level of theory. This is probably reflecting the subtle differences in the potential energy surface at different levels of theory, particularly in the inclusion of the electron correlation.

In Table 3 we have collected the NBO charges obtained at the QCISD/6-311+G(d) level for the different MC_2^+ species. It can be readily seen that NBO charges at the metal are quite close for both linear and cyclic isomers. Only in the case of NiC_2^+ a difference larger than 0.2e is found between the metal charges for both isomers. The general observation is that the positive charge is mainly located at the metal atom. This is obviously an expected result given the higher ionization potential of dicarbon (11.4 eV[53]) than any of the first-row transition metals. In addition, the relatively large charge at the metal atom found in most cases indicates that there is also a net transfer of electronic charge density from the metal toward the C_2 unit. We will come to this point later.

So far we are distinguishing between *linear* and *cyclic* isomers. However, what we are calling *cyclic* MC_2^+ species can be in fact of two different types, depending on the connectivity between the atoms. They could be truly cyclic isomers, with two individual M−C bonds, or T-shaped species, with essentially M−C_2 bonding, that is, with the metal bonded to the entire C_2 unit. In order to analyze the type of interaction in MC_2^+ compounds, we have applied a topological analysis of the electronic charge density.[47] A summary of the results obtained by employing the QCISD/6-311+G(d) electronic density is shown in Table 4. In our case only bond critical points (corresponding to a minimum value of $\rho(r)$ along the line linking

TABLE 4: Summary of Critical Point Data for the Linear and Cyclic Isomers of MC_2^+ Species[a]

type		Sc	Ti	V	Cr	Mn	Fe	Co	Ni	Cu	Zn
						Linear Isomer					
M−C bond	$\rho(r)$	0.1626	0.1555	0.1074	0.1204	0.1116	0.1266	0.1238	0.1385	0.1221	0.1241
	$\nabla^2\rho(r$	0.2365	0.2091	0.3453	0.3268	0.2837	0.3720	0.3204	0.4786	0.4078	0.3641
	$-H(r)$	0.1490	0.1352	0.1234	0.1274	0.1126	0.1386	0.1202	0.1596	0.1284	0.1206
C−C bond	$\rho(r)$	0.3576	0.3282	0.3656	0.3656	0.3714	0.3693	0.3520	0.3492	0.3483	0.3728
	$\nabla^2\rho(r)$	−1.1298	−0.8739	−1.0105	−1.0017	−1.0102	−1.0387	−1.1316	−0.9903	−0.9437	−0.9890
	$-H(r)$	0.1685	0.1882	0.2671	0.2665	0.2884	0.2668	0.1522	0.2068	0.2095	0.2813
						Cyclic Isomer					
M−C_2 bond	$\rho(r)$	0.1180	0.1273	0.1444[b]	0.1422	0.0790	0.0881	0.1086	0.1112	0.0932[b]	0.0845
	$\nabla^2\rho(r)$	0.2943	0.3091		0.3796	0.2459	0.3684	0.3521	0.4165		0.2865
	$-H(r)$	0.1189	0.1298		0.1557	0.0831	0.1136	0.1211	0.1321		0.0852
M−C bond	$\rho(r)$			0.1446						0.0937	
	$\nabla^2\rho(r)$			0.4321						0.2938	
	$-H(r)$			0.1728						0.0943	
C−C bond	$\rho(r)$	0.3756	0.3736	0.3447	0.3377	0.3451	0.3475	0.3507	0.3512	0.3383	0.3444
	$\nabla^2\rho(r)$	−1.1251	−1.1231	−0.9472	−0.9125	−0.9351	−0.9348	−0.9822	−0.9840	−0.9679	−0.9519
	$-H(r)$	0.2234	0.2194	0.2013	0.1881	0.2078	0.2141	0.2046	0.2059	0.1681	0.2000

[a] Critical point data, calculated by use of the QCISD/6-311+G(d) electronic density, are given in atomic units. [b] Electronic density value for the ring critical point.

the nuclei and a maximum along the interatomic surfaces) and ring critical points [$\rho(r)$ being a minimum in two directions and a maximum in one direction] are relevant. Important properties of critical points in order to identify the nature of the interaction are the electronic density $\rho(r)$, the Laplacian of the electronic density $\nabla^2\rho(r)$, and the total energy density $H(r)$ at the critical point.

It can be seen in Table 4 that most MC_2^+ *cyclic* isomers are in fact T-shaped species, since only M−C_2 bond critical points are found. Only in the cases of VC_2^+ and CuC_2^+ is a true ring found, since two individual M−C bonds and a ring critical point are found in each case. However, it should be noted that the $\rho(r)$ values at the ring and bond critical points for these two species are very close. Furthermore, the ring critical point is only 0.156 Å (V) and 0.210 Å (Cu), respectively, apart from the bond critical point. Therefore, in cyclic VC_2^+ and CuC_2^+ the individual M−C bonds are rather curved, and they approach very much a T-shaped description. Consequently, we may conclude from the data shown in Table 4 that nonlinear MC_2^+ isomers are best described as T-shaped species. Nevertheless, in what follows we will continue referring to these species indistinctly as cyclic or T-shaped isomers.

Analysis of the electronic density also helps to characterize the type of the interaction between atoms in a molecule.[47] Basically, two limiting types of interactions can be distinguished. Shared interactions (typical of covalent bonds) are characterized essentially by large electronic densities and negative values of its Laplacian. For example, all C−C bonds in MC_2^+ compounds, as can be seen in Table 4, are clearly shared interactions. On the other hand, closed-shell interactions (typical of ionic compounds and van der Waals complexes) have relatively low $\rho(r)$ values and positive values of its Laplacian. All M−C bonds have these characteristics, and in principle they should be classified as closed-shell interactions. However, it has been suggested[54,55] that the total energy density, $H(r)$, might be indicative of the degree of covalency of an interaction: negative $H(r)$ values (indicating that the system is stabilized by accumulation of electronic charge) are associated with covalent interactions,[55] whereas positive $H(r)$ values (accumulation of electronic charge destabilizes the system) are characteristic of noncovalent interactions. The $H(r)$ values for M−C interactions shown in Table 4, which are negative in all cases, suggest that all M−C bonds have a certain degree of covalency. Therefore, the M−C interactions in MC_2^+ compounds should be classified as intermediate, with typical characteristics of ionic bonds [low $\rho(r)$, positive Laplacian] but at the same time with some covalent features (negative total energy at the bond critical point).

TABLE 5: Relative Energies for MC_2^+ Species at Different Levels of Theory[a]

	level			
	B3LYP	QCISD	CCSD(T)	MRCI[b]
ScC_2^+ ($^1\Sigma^+$, $^1A_1$)	−21.44	−27.49[a]	−27.01[a]	−23.81[a]
TiC_2^+ ($^2\Delta$, $^2A_2$)	−18.73	−25.00	−28.29	−19.82
VC_2^+ ($^5\Delta$, $^3B_1$)	−13.33	−15.48	−15.78	−14.38
CrC_2^+ ($^6\Sigma^+$, $^4B_1$)	−5.58	+3.48	−4.02	−1.66
MnC_2^+ ($^7\Sigma^+$, $^5A_1$)	−2.07	−4.66	−6.62	−5.69
FeC_2^+ ($^6\Delta$, $^6A_1$)	−3.33	−4.55	−6.45	−3.44
CoC_2^+ ($^5\prod$, $^5A_2$)	−5.73	−8.10	−9.98	−11.15
NiC_2^+ ($^4\Sigma^-$, $^4A_2$)	−5.68	−0.68	−7.25	−11.46
CuC_2^+ ($^3\prod$, $^3B_1$)	+2.08	+1.48	+1.18	+4.01
ZnC_2^+ ($^2\Sigma^+$, $^2A_1$)	−4.59	−4.04	−6.11	−1.47

[a] Relative energies ($E_{cyclic} - E_{linear}$), calculated with the 6-311+G(3df) basis set and including ZPV corrections, are given in kilocalories per mole. In the case of QCISD, CCSD(T), and MRCI calculations, QCISD/6-311+G(d) ZPVE values have been employed. [b] MRCI calculations were done with the 6-311+G(d) basis set. [c] ZPV energies for the linear isomer were computed at the QCISD/LAN-G+(d) level.

Linear−Cyclic Competition. In this section we will address the competition between both MC_2^+ isomers, linear and cyclic (T-shaped). The relative energies of both isomers are given in Table 5, whereas the variation of the energy of the system with the angle (φ) formed by the line connecting the metal with the middle point of C_2 and the C−C bond is shown in Figure 1 (Sc−Mn in panel a and Fe−Zn in panel b). The curves have been obtained representing the CCSD(T)/6-311+G(d) energy computed at the optimized B3LYP/6-311+G(d) geometries for fixed values of the φ angle. This kind of representation has proved useful in the analysis of other related systems, such as the neutral transition-metal dicarbides[32] and second-row main-group dicarbides.[56]

A first glance at Figure 1 reveals that MC_2^+ systems have in general a clear preference for cyclic arrangements. The only exception is CuC_2^+, where it seems that the preferred arrangement is the linear one. As a general rule, the variation of the energy is more pronounced for early transition metals, with an almost regular decrease in the depth of the cyclic well from Sc to Mn. Late transition metal dicarbides (perhaps with the exception of Co) exhibit a rather small variation of the energy

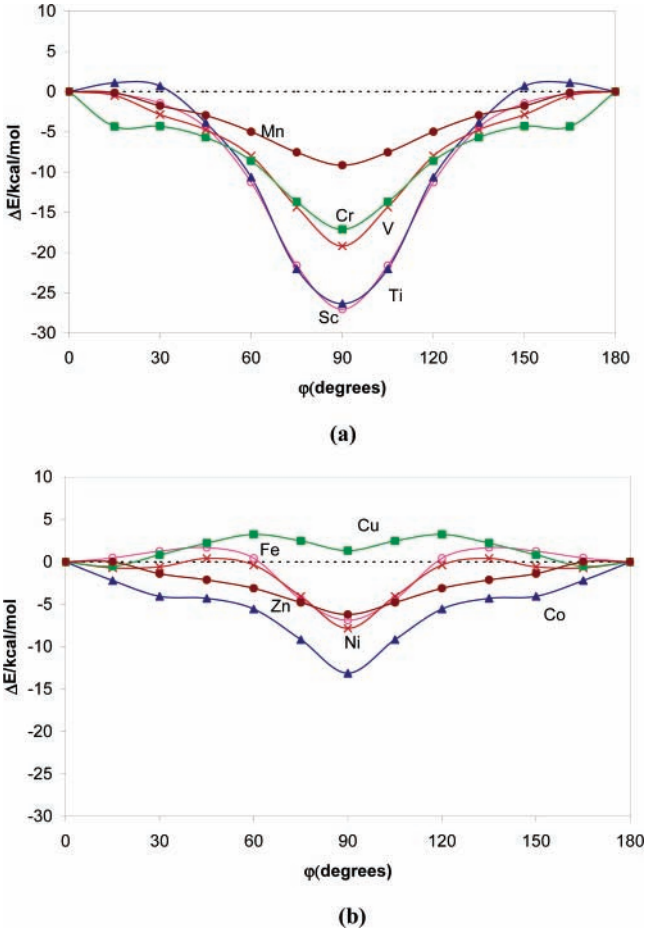

Figure 1. Variation of the total energy (in kilocalories per mole, relative to the linear geometry), computed at the CCSD(T)/6-311+G-(d) level, for the different MC_2^+ compounds with the angle (φ) between the line connecting the M atom and the middle point of the C−C bond. Panel a corresponds to the early transition metals (Sc−Mn), whereas in panel b the results for late transition metals (Fe−Zn) are represented.

with the geometry of the system, especially in the case of CuC_2. Another interesting feature of the graphs shown in Figure 1 is that in all cases they suggest very small potential barriers for interconversion between both isomers. Barriers for isomerization between the linear (when this is a minimum) and cyclic species are always below 2 kcal/mol. Therefore, the possibility of simultaneously detecting both isomers in eventual experimental searches seems to be very low.

A special case is CuC_2^+, where the linear isomer is more stable. The barrier for the cyclic−linear isomerization seems to be also of the same magnitude, 2 kcal/mol, as for the rest of the late transition metal MC_2^+ compounds. But the most salient feature of CuC_2^+ is its very flat potential surface. It is very economic, in terms of energy, to modify the geometry of the molecule. Therefore, this is a clear case of a polytopic system.[57] Polytopic systems are those with very flat potential surfaces, suggesting the possibility of a pinwheel motion of an atom or ion around a molecular fragment.[57] Examples of polytopic systems can be found within carbides. A prototypical case is SiC_2, which has been found to exhibit a very flat potential surface with the T-shaped isomer being slightly more stable than the linear one.[58] It seems that in the case of SiC_2 the balance between ionic and covalent interactions, favoring the cyclic and linear arrangements, respectively, is the origin of such polytopism.[56]

The energy differences between linear and cyclic species computed at higher levels of theory are shown in Table 5. These values confirm the previous discussion based on the variation of the energy with the geometry. The cyclic (T-shaped) isomer is always found to be the predicted global minimum, with the single exception of CuC_2^+. The energy difference is relatively high for early transition metals, such as Sc or Ti, with values around 27−28 kcal/mol at the CCSD(T) level. The cyclic−linear relative energy is moderate for V (around 15 kcal/mol), and the rest of the transition metals have values within 4−9 kcal/mol. In the case of CuC_2^+, the energy difference is very small, just about 1 kcal/mol. CuC_2^+ seems in fact a good candidate for a possible experimental detection of both isomers, linear and cyclic, since both are shown to be true minima on the potential surface and of similar stability.

An interesting conclusion from the results shown in Table 5 is the very good behavior of the B3LYP method predicting the relative stability of linear and cyclic isomers for MC_2^+ compounds. All B3LYP relative energies are in very good qualitative, and even quantitative, agreement with the CCSD-(T) values. Only for CuC_2^+ is a difference of nearly 10 kcal/mol between B3LYP and CCSD(T) values observed, but its overall performance seems to be better than QCISD, for example.

Analysis of Bonding in MC_2^+ Cations. In this section we will address the analysis of bonding in the MC_2^+ complexes. Let us start by comparing the electronic structure of the dicarbide cations of first-row transition metals to that of their neutral parents MC_2. We remind the reader that the electronic configuration of dicarbon in its ground electronic state $X^1\Sigma_g^+$ ($1\sigma_g^2$ $1\sigma_u^2$ $2\sigma_g^2$ $2\sigma_u^2$ $1\pi_u^4$ $3\sigma_g^0$) makes it a singular molecule with no formal σ contribution to its bond order of 2. The empty $3\sigma_g$ orbital lies, however, very close in energy to the $1\pi_u$ orbital. This makes dicarbon an extremely good σ-acceptor ligand with an electron affinity of 3.273 eV.[53] When it is taken also into account that the ground electronic configuration of the first-row transition metals is s^2d^n (except for Cr and Cu), the electronic structure of neutral MC_2 can be described in terms of donor−acceptor interactions,[32] namely, σ donation from the metal 4s orbital to the C_2 unit and π back-donation from the dicarbide to the empty dπ orbitals of the metal (for a detailed description of such interactions, see ref 32). Besides, the d nonbonding electrons fill first the δ-type orbitals (which have the lowest M−C_2 overlap) and then the π antibonding orbitals. It is expected that σ donation contributes more to the bond energy than the π back-donation due to both the low-lying character of the $3\sigma_g$ lowest unoccupied molecular orbital (LUMO) in C_2 and the high-lying character of metal π orbitals, which are, furthermore, either single- or double-occupied in all cases except for Sc, Ti, and V. In cyclic (C_{2v}) isomers, the in-plane $\pi_{||}$ orbital of C_2 belongs to the same representation as the 4s, $3d_{z^2}$, and $3d_{x^2-y^2}$ metal orbitals. Nevertheless, the bonding situation can also be described in terms of charge donation from the metal 4s orbital into the LUMO of C_2 (accompanied by charge redistribution among the $\pi_{||}$, $3d_{z^2}$, and $3d_{x^2-y^2}$ orbitals) and back-donation from the dicarbide through its $\pi_\perp$ orbital. From this bonding picture it would be expected that ground states of transition metal dicarbides have the same spin symmetry as their constituent metal atoms, and this is actually what is found[32] (the only exceptions are CrC_2 species, which correlate with $Cr(^7S) + C_2(^3\Pi_u)$ and have $S = 2$).

When the electronic ground states of the neutral dicarbides are kept in mind,[32] it is relatively straightforward to obtain the ground state terms of the cations. In the linear isomers, the additional electron is always removed from the 11σ orbital [which is either the highest occupied molecular orbital (HOMO)

TABLE 6: Dissociation Energies for Linear and Cyclic MC_2^+ Species[a]

	linear		cyclic	
	B3LYP	CCSD(T)	B3LYP	CCSD(T)
ScC_2^+ ($^1\Sigma^+$, $^1A_1$)	105.74	97.77[b]	127.18	124.78
TiC_2^+ ($^2\Delta$, $^2A_2$)	97.81	83.98	116.54	112.27
VC_2^+ ($^5\Delta$, $^3B_1$)	97.64	71.26	87.75	88.72
CrC_2^+ ($^6\Sigma^+$, $^4B_1$)	78.48	50.05	60.84	51.72
MnC_2^+ ($^7\Sigma^+$, $^5A_1$)	93.85	60.63	72.69	68.94
FeC_2^+ ($^6\Delta$, $^6A_1$)	104.57	69.28	107.91	75.73
CoC^{2+} ($^5\Pi$, $^5A^2$)	64.09	57.18	64.10	57.19
NiC^{2+} ($^4\Sigma^-$, $^4A^2$)	54.42	46.24	60.10	53.94
CuC^{2+} ($^3\Pi$, $^3B^1$)	47.44	36.18	45.36	35.00
ZnC^{2+} ($^2\Sigma^+$, $^2A^1$)	53.35	58.14	57.94	64.25

[a] Dissociation energies at the B3LYP and CCSD(T) levels of theory, including ZPVE corrections, with the 6-311+G(3df) basis set are given in kilocalories per mole. In the case of CCSD(T) calculations, QCISD/6-311+G(d) ZPVE values have been employed. [b] ZPV energies were computed at the QCISD/LAN-G+(d) level.

or the next-HOMO], yielding terms with the same spatial symmetry as those of their neutral parents. There are two exceptions, namely, CrC_2^+ and CuC_2^+, where the additional electron is removed from π (antibonding) orbitals (CrC_2 is the first compound within the row to include metal dπ electrons and CuC_2 is the first compound to fill the dπ orbitals). Besides, from Co to Zn the additional electron is removed from a filled orbital and the spin symmetry of the cation is therefore increased in one unit with respect to that of the neutral. From Sc to Fe the additional electron is removed from a half-filled orbital and the spin symmetry of the cation is reduced in one unit. In the latter case, it is possible for MC_2^+ to uncouple two electrons, increasing the exchange interactions among the metal electrons (but weakening the metal ligand bond). This is what happens in fact in VC_2^+, CrC_2^+, MnC_2^+, and FeC_2^+. On the contrary, in ScC_2^+ and TiC_2^+, where the number of d electrons is small, the exchange effects are much less important and bonding considerations favor low spin symmetries.

In the C_{2v} isomers the situation is also relatively straightforward, for in most cases the spin and spatial symmetries of the cations MC_2^+ are the same as for the isoelectronic neutrals. The exceptions are TiC_2^+, VC_2^+, and NiC_2^+, where a different state is found to be slightly lower in energy. At variance with linear isomers, from Sc to Mn all cyclic isomers have lower spin symmetries than their neutral parents.

To summarize, when comparing the electronic structures of neutral and cationic transition metal dicarbides, we find that linear MC_2^+ isomers remove the additional electron from the nonbonding 11σ orbital of MC_2, whereas cyclic cationic isomers tend to adopt the same electronic configuration as their isoelectronic neutrals. Furthermore, linear isomers from the middle of the transition row are prone to increase their spin symmetry, maximizing the exchange interactions. This is at variance with cyclic isomers, which displays in all cases low spin symmetries.

In order to analyze the relative stability of the different MC_2^+ cations, it is useful to compute their dissociation energies. The dissociation energies, toward their respective dissociation limits, of MC_2^+ compounds at the B3LYP and CCSD(T) levels of theory are given in Table 6. A reasonable agreement between both levels of theory is observed for those compounds dissociating to $M^+ + C_2$ ($^3\Pi_u$). On the other hand, in those cases where the correlating asymptote is $M^+ + C_2$ ($^1\Sigma_g^+$), the agreement is usually poorer. The main reason for this fact is the poor description of C_2 ($^1\Sigma_g^+$) at the B3LYP level, which is placed 23 kcal/mol higher in energy than C_2 ($^3\Pi_u$). It seems that a proper incorporation of correlation effects is required for a good description of the $^1\Sigma_g^+$ ground state of dicarbon.[59,60] In fact, the accessible 3σ_g orbital provides a certain multireference character to its ground state, although this ground state is dominated by the previously mentioned configuration. A general trend observed in Table 6 is that early transition metal (Sc, Ti) MC_2^+ cations have the largest dissociation energies. In fact, these two systems show dissociation energies very close to their neutral analogues.[32] ZnC_2^+ has also a comparable (even larger) dissociation energy than its neutral counterpart, ZnC_2, although the absolute value is nearly half the dissociation energy of ScC_2^+.

Let us now discuss the electronic structure of cationic transition metal dicarbides in terms of their dissociating fragments. These will be in all cases M^+ and C_2 because the ionization energy of the dicarbide molecule, 11.4 eV,[53] is clearly larger than that of the metals. The ground-state electronic configurations of the first-row transition metal cations are d^ns^1 (Sc, Ti, Mn, Fe, and Zn) and $d^{n+1}s^0$ (V, Cr, Co, Ni, and Cu). We also remind the reader that dicarbon has a low-lying $^3\Pi_u$ excited state ($1\sigma_g^2\ 1\sigma_u^2\ 2\sigma_g^2\ 2\sigma_u^2\ 1\pi_u^3\ 3\sigma_g^1$) only 716 cm^{-1} above the ground state.[53] We will begin the analysis of the electronic structure of the title systems with the linear isomers (from now on, and unless otherwise specified, QCISD/6-311+G(3df) geometries and CCSD(T)/6-311+G(3df) energies will be discussed).

The ground electronic state of ScC_2^+ is $^1\Sigma^+$ ($...3\pi^4 10\sigma^2$), which correlates with the Sc^+ (^{3}D; d^1s^1) + C_2 ($^3\Pi_u$) asymptote. The $^3\Delta$ state ($...3\pi^4 10\sigma^1 1\delta^1$), which correlates to the ground-state fragments Sc^+ (^{3}D; d^1s^1) + C_2 ($^1\Sigma_g^+$), lies about 15 kcal/mol higher in energy due to weaker bonding interactions that are not compensated by the retaining of the small s−d exchange energy. With respect to the ground-state configuration of ScC_2^+, for TiC_2^+ and VC_2^+ the additional electrons add to the δ orbitals, leading to $^2\Delta$ ($...3\pi^4 10\sigma^2 1\delta^1$) and $^3\Sigma^-$ ($...3\pi^4 10\sigma^2 1\delta^2$) states, respectively, which correlate to the Ti^+ (^{4}F; d^2s^1) + C_2 ($^3\Pi_u$) and V^+ (^{5}D; d^4) + C_2 ($^3\Pi_u$) asymptotes. The dissociation energies of TiC_2^+ ($^2\Delta$) and VC_2^+ ($^3\Sigma^-$) decrease with respect to ScC_2^+ ($^1\Sigma^+$) by 13.8 and 29.2 kcal/mol, respectively. This should be related to the increasing loss of exchange energy in the transition metal cation as we move on in the row. In the particular case of VC_2^+, with d^4s^0 ground electronic configuration in V^+, we expect exchange effects to be especially important because the energy loss is larger for d−d exchange than for s−d exchange. We have therefore investigated the quintet states of V^+ where all four electrons remain high-spin-coupled and no exchange energy is lost. The lowest-lying quintet is $^5\Delta$ ($...10\sigma^1 1\delta^1 4\pi^2$), which correlates to the V^+ (^{5}D; d^4) + C_2 ($^1\Sigma_g^+$) asymptote. The balance between bonding and exchange effects in VC_2^+ seems to be delicate, for theory predicts both states ($^3\Sigma^-$, $^5\Delta$) to be nearly degenerate [at the CCSD(T) level the $^5\Delta$ state is only 3 kcal/mol lower; at the MRCI level both are within 1 kcal/mol, which is obviously below the precision of our calculation]. We have adopted in our calculations the $^5\Delta$ state, which is the lowest-lying one at the CCSD(T) level. The species CrC_2^+ and MnC_2^+ have $^6\Sigma^+$ ($...10\sigma^1 1\delta^2 4\pi^2$) and $^7\Sigma^+$ ($...10\sigma^1 1\delta^2 4\pi^2 11\sigma^1$) high-spin ground states [with respect to VC_2^+ ($^5\Delta$), the additional electrons added to the open-shell 1δ and the empty 11σ orbitals]. These states correlate to the Cr^+ (^{6}S; d^5) + C_2 ($^1\Sigma_g^+$) and Mn^+ (^{7}S; d^5s^1) + C_2 ($^1\Sigma_g^+$) asymptotes, respectively. Due to the five high-spin-coupled electrons in CrC_2^+, exchange effects dominate over bonding considerations and the high-spin $^6\Sigma^+$ state lies 16 kcal/mol below the most stable quartet $^4\Sigma^-$. For MnC_2^+ the lowest quintet is $^5\Sigma^+$, which

correlates to the $Mn^+[^5S; d^5(^6S)s^1] + C_2 (^1\Sigma_g^+)$ asymptote. Notice that for MnC_2^+ no exchange energy is lost upon formation of the complex, either in the $^7\Sigma^+$ state or in the $^5\Sigma^+$ state, because both correlate to dicarbon in its singlet state. However, MnC_2^+ $^5\Sigma^+$ requires the promotion of the metal to its ^5S state, which lies about 27 kcal/mol higher than the ground-state ^7S. On the other hand, bonding considerations favor MnC_2^+ $^5\Sigma^+$ with a formal σ bond order of 1. The balance between these effects is again delicate, for both CCSD(T) and MRCI predict $^5\Sigma^+$ to be almost isoenergetic with $^7\Sigma^+$ (at the MRCI level, $^7\Sigma^+$ is more stable by 5 kcal/mol). The bonding situation in VC_2^+ ($^5\Delta$) and CrC_2^+ ($^6\Sigma^+$) is very similar, however, the dissociation energy decreases by 20 kcal/mol from V to Cr. The CASSCF population of the 4s and 3d orbitals for the two species is $4s^{0.61}$ $3d_\sigma^{0.22}$ $3d_\pi^{2.06}$ $3d_\delta^{1.0}$ and $4s^{0.74}$ $3d_\sigma^{0.27}$ $3d_\pi^{2.06}$ $3d_\delta^{2.0}$, respectively. Notice the larger population of the 4s orbital with respect to the $3d_\sigma$, suggesting a strong mixing with the excited V^+ [^5F; $d^3(^4F)s^1$] and Cr^+ [^6D; $d^4(^5D)s^1$] states. These states are probably favored by bonding considerations, for the 4s orbital has a larger radius that allows better overlap with the orbitals of the C_2 moiety (more specifically, with the $2\sigma_u$ and $3\sigma_g$ orbitals). We can now tentatively explain the observed decrease in the dissociation energy from V to Cr in terms of the relative energies of the dissociating asymptotes: whereas $V^+ (^5F) + C_2 (^1\Sigma_g^+)$ lies only 8 kcal/mol higher than $V^+ (^5D) + C_2 (^1\Sigma_g^+)$, $Cr^+ (^6D) + C_2 (^1\Sigma_g^+)$ lies 35 kcal/mol higher than $Cr^+ (^6S) + C_2 (^1\Sigma_g^+)$. The larger binding energy of MnC_2^+ with respect to CrC_2^+ ($^6\Sigma^+$) is reasonable if it is taken into account that the additional electron adds to a σ bonding orbital.

With respect to the electronic configuration of MnC_2^+ $^5\Sigma^+$, for FeC_2^+ the additional electron now adds to the already doubly occupied 1δ orbital, leading to the $...10\sigma^1 1\delta^3 4\pi^2 11\sigma^1$, $^6\Delta$, ground state, which correlates with the $Fe^+ (^6D; d^6s^1) + C_2 (^1\Sigma_g^+)$ asymptote. The electronic structure is very similar to that previously described for MnC_2^+, and thus we observe similar dissociation energies. For the rest of the metals the additional electron adds successively to 10σ, 1δ (now fully occupied), 4π, and again 4π, leading to the following ground states and electronic configurations: CoC_2^+, $^5\Delta$ ($...10\sigma^2 1\delta^3 4\pi^2 11\sigma^1$); NiC_2^+, $^4\Sigma^-$ ($...10\sigma^2 1\delta^4 4\pi^2 11\sigma^1$); CuC_2^+, $^3\Pi$ ($...10\sigma^2 1\delta^4 4\pi^3 11\sigma^1$); and ZnC_2^+, $^2\Sigma^+$ ($...10\sigma^2 1\delta^4 4\pi^4 11\sigma^1$). Except ZnC_2^+, which correlates to $Zn^+ (^2S; d^{10}s^1) + C_2 (^1\Sigma_g^+)$, they all correlate to their ground atomic states and dicarbon in its first excited state, namely, $Co^+(^3F; d^8) + C_2 (^3\Pi_u)$, $Ni^+ (^2D; d^9) + C_2 (^3\Pi_u)$, and $Cu^+ (^1S; d^{10}) + C_2 (^3\Pi_u)$. We assign the steady decrease observed in the dissociation energy from Fe to Ni to mixing with the asymptote $TM^+ (d^ns^1) + C_2 (^1\Sigma_g^+)$. The CASSCF population of the 4s and 3d orbitals for these species is $4s^{1.2}$ $3d^{6.1}$ (for Fe^+, whose ground state is d^ns^1), $4s^{1.1}$ $3d^{7.1}$ (for Co), and $4s^{0.66}$ $3d^{8.2}$ (for Ni). With respect to the $d^{n+1}s^0$ ground state, the $TM^+ (d^ns^1) + C_2 (^1\Sigma_g^+)$ asymptote lies about 12 and 27 kcal/mol higher for Co^+ and Ni^+, respectively. On the other hand, the bonding situation of CuC_2^+ is very poor with a fully occupied d-shell and the $TM^+ (d^ns^1) + C_2 (^1\Sigma_g^+)$ asymptote lying 65 kcal/mol higher in energy. This explains its low dissociation energy. The additional electron in ZnC_2^+ ($^2\Sigma^+$) adds, however, to a binding σ orbital, increasing the dissociation energy again.

Let us turn now to the C_{2v}-symmetry species. We begin by pointing out that in all cases except FeC_2^+ and ZnC_2^+, the ground electronic states correlate to ground-state cations and C_2 ($^3\Pi_u$). Therefore, we will not indicate in what follows which one is the dissociating asymptote unless necessary. Cyclic ScC_2^+ has $^1A_1$ ground state with the following electron configuration ... $8a_1^2 3b_1^2 9a_1^2$ and a very similar bonding situation compared to its linear isomer $^1\Sigma^+$. For TiC_2^+ the additional electron adds to the $1a_2$ ($3d_{xy}$) nonbonding orbital, yielding a $^2A_2$ ground state. For VC_2^+ ($^3B_1$) the extra electron adds to the b_2 ($3d_{yz}$) orbital, which has the same symmetry as the empty $\pi_\parallel$* orbital of the C_2 fragment. For CrC_2^+ ($^4B_1$) and MnC_2^+ ($^5A_1$) the additional electrons add to the nonbonding $10a_1$ and the $4b_1$ orbitals, respectively. From Sc to Cr, the dissociation energies decrease as expected due to the exchange energy loss. For all these species we have searched for states of higher multiplicity, but all of them lie higher in energy than the ground low-spin states described above. This is at variance with what happened in the VC_2^+, CrC_2^+, and MnC_2^+ linear isomers, where states of higher spin symmetry were more stable. It therefore seems that for these systems chemical bonding considerations dominate over exchange effects. This is probably related to the better overlap between the a_1 metal orbitals and the dicarbide $3\sigma_g$ LUMO in the C_{2v} symmetry. It must be pointed out that the energetic differences between the low- and high-spin states is very small and decreases as the number of d electrons increases: CrC_2^+ ($^6\Sigma^+$) lies about 6 kcal/mol higher than CrC_2^+ ($^4\Sigma^-$), whereas MnC_2^+ ($^7A_1$) and MnC_2^+ ($^5A_1$) are almost degenerate.

The addition of electrons from FeC_2^+ to ZnC_2^+ is quite straightforward. For FeC_2^+ ($^6A_1$) it adds to the still-empty $11a_1$ orbital, and from Co on the extra electrons add in such a way that they fill first nonbonding orbitals and then the π orbitals: for CoC_2^+ ($^5A_2$) it adds to the $1a_2$; for NiC_2^+ ($^4A_2$), to the $10\ a_1$; for CuC_2^+ ($^3B_1$), to the $5b_2$; and finally, for ZnC_2^+ ($^2A_1$), to the $4b_1$. The steady decrease in the dissociation energy from Fe to Cu as well as the increase in Zn can be explained in terms of mixing with the lowest excited asymptote, as mentioned above.

We finish this section by commenting briefly on the conformational preference between cyclic or linear conformations in these systems. On the one hand, it seems clear that electrostatic arguments favor a cyclic arrangement since the leading electrostatic term is the charge−quadrupole interaction and the quadrupole moment of C_2 is positive. Furthermore, interaction of metal valence orbitals with $3\sigma_g$ should be slightly more favored in C_{2v} symmetry due to the larger overlapping between the corresponding orbitals. These qualitative arguments should explain then the clear conformational preference for the cyclic structures found in ScC_2^+, TiC_2^+, VC_2^+, CoC_2^+, and NiC_2^+. For the rest of the systems, although cyclic isomers seem to be favored over the linear ones (with the possible exception of CuC_2^+; see Table 5), the energetic difference between them is small and we do not think that it can be explained only in terms of qualitative arguments.

Finally, we have computed the adiabatic ionization energies of MC_2 dicarbides. The results at the CCSD(T)/6-311+G(3df) level are given in Table 7, along with the theoretical [at the CCSD(T) level] and experimental[61] values for the corresponding transition metals. It can be observed that cyclic species have slightly larger ionization potentials than the linear ones, with the exceptions of ScC_2, TiC_2, and ZnC_2. Nevertheless, the most significant feature of ionization energies of first-row transition metal dicarbides is that they are close to the metal ionization potentials, following in general the same trend, increasing slightly as the atomic number increases, although with small oscillations along the series. This result further confirms that the electron is essentially lost in the transition metal.

Conclusions

A theoretical study of the first-row transition metal dicarbide cations MC_2^+ (M = Sc−Zn) has been carried out. Different

TABLE 7: Ionization Potentials for Linear and Cyclic MC_2 Species[a]

	linear	cyclic	metal (theor)	metal (exptl)[b]
ScC_2 ($^2\Sigma^+$, $^2A_1$)	6.84	6.46	6.34	6.561 44
TiC_2 ($^3\Delta$, $^3B_2$)	7.39	6.93	6.61	6.8282
VC_2 ($^4\Sigma^-$, $^4B_1$)	7.49	7.92	6.56	6.746
CrC_2 ($^5\Pi$, $^5A_1$)	7.64	8.42	6.46	6.766 64
MnC^2 ($^6\Sigma^+$, $^6A_1$)	7.76	8.12	7.25	7.434 02
FeC_2 ($^5\Delta$, $^5A_2$)	8.08	8.57	7.71	7.9024
CoC_2 ($^4\Delta$, $^4B_1$)	8.38	8.84	7.57	7.8810
NiC_2 ($^3\Sigma^-$, $^3B_1$)	9.10	9.35	7.25	7.6398
CuC_2 ($^2S^+$, $^2A_1$)	9.35	9.70	7.43	7.726 38
ZnC_2 ($^1\Sigma^+$, $^1A_1$)	8.83	8.79	9.13	9.394 05

[a] Ionization potentials at the CCSD(T) level of theory, including QCISD/6-311+G(d) ZPVE corrections, with the 6-311+G(3df) basis set are given in electronvolts. Theoretical [CCSD(T) level] and experimental IPs for the different transition metals are also given in electronvolts. [b] Reference 61.

molecular properties that could help in their eventual experimental detection, such as geometries and vibrational frequencies, have been computed. It has been found that most MC_2^+ compounds prefer a C_{2v}-symmetric arrangement over the linear geometry. In particular, for early transition metals, the C_{2v} isomer is particularly favored over the linear one, with energy differences between the two isomers of 27−28 kcal/mol for ScC_2^+ and TiC_2^+. For the rest of the series the cyclic isomer lies about 4−9 kcal/mol below the linear species. Therefore, it seems that early transition metal cations have a greater tendency to bond to both carbon atoms (forming a C_{2v}-symmetric species) than late transition metal cations. CuC_2^+ is a special case, since the linear isomer is predicted to be the global minimum, although the C_{2v} isomer lies only about 1 kcal/mol higher in energy. In fact, the potential surface for CuC_2^+ is very flat, with energy differences lower than 2 kcal/mol for the movement of the metal around the C_2 moiety, conferring on this system a polytopic character. In all cases the isomerization barrier between linear and cyclic species seems to be very small (below 2 kcal/mol), and therefore interconversion between them should be rather facile. The topological analysis of the electronic density shows that in most cases the C_{2v} isomer is in fact a T-shaped structure, with the metal bonded to the entire C_2 unit. Only for VC_2^+ and CuC_2^+ does the C_{2v}-symmetric isomer corresponds to a true ring structure with peripheral M−C bonds. However, even in those cases the M−C bonds are rather curved and the structure approaches a T-shaped description. In general, MC_2^+ compounds for early transition metals have larger dissociation energies than those formed by late transition metals. In most cases the dissociation energies for MC_2^+ compounds are considerably smaller than those obtained for their neutral analogues.

A detailed analysis of the bonding in MC_2^+ compounds has been carried out. It has been shown that the different interactions between the corresponding fragments, M^+ and C_2, may help to explain most of the properties of MC_2^+ cations.

Acknowledgment. This research has been supported by the Ministerio de Ciencia y Tecnología of Spain (Grant CTQ2004-07405-C02-01) and by the Junta de Castilla y León (Grant VA 085/03). V.M.R. gratefully ackowledges funds from the Ministerio de Educación y Ciencia within the Ramón y Cajal Program and cofunding from the Fondo Social Europeo (Programa Operativo Integrado FEDER-FSE,2000/2006).

Supporting Information Available: Complete refs 45 and 46, IR frequencies and intensities for linear and cyclic species (Tables S1 and S2), and leading CASSCF CI coefficients (0.1 cutoff; Table S3). This material is available free of charge via the Internet at http://pubs.acs.org.

References and Notes

(1) Guo, B. C.; Kearns, K. P.; Castleman, A. W. *Science* **1992**, *255*, 1411.
(2) Guo, B. C.; Wei, S.; Purnell, J.; Buzza, S.; Castleman, A. W. *Science* **1992**, *256*, 515.
(3) Wei, S.; Guo, B. C.; Purnell, J.; Buzza, S.; Castleman, A. W. *Science* **1992**, *256*, 818.
(4) Wei, S.; Guo, B. C.; Purnell, J.; Buzza, S.; Castleman, A. W. *J. Phys. Chem.* **1992**, *96*, 4166.
(5) Pilgrim, J. S.; Duncan, M. A. *J. Am. Chem. Soc.* **1993**, *115*, 6958.
(6) Rohmer, M. M.; Benard, M.; Poblet, J. M. *Chem. Rev.* **2000**, *100*, 495.
(7) van Heijnsbergen, D.; Duncan, M. A.; Meijer, G.; von Helden, G. *Chem. Phys. Lett.* **2001**, *349*, 220.
(8) Dance, I. J. *J. Am. Chem. Soc.* **1996**, *118*, 2699.
(9) Dance, I. J. *J. Am. Chem. Soc.* **1996**, *118*, 6309.
(10) Poblet, J. M.; Rohmer, M. M.; Benard, M. *Inorg. Chem.* **1996**, *35*, 4073.
(11) Hou, H.; Muckerman, J. T.; Liu, P.; Rodriguez, J. A. *J. Phys. Chem. A* **2003**, *107*, 9344.
(12) Wang, L. S.; Li, S.; Wu, H. *J. Phys. Chem.* **1996**, *100*, 19211.
(13) Li, S.; Wu, H.; Wang, L. S. *J. Am. Chem. Soc.* **1997**, *119*, 7417.
(14) Chai, Y.; Guo, T.; Jin, C.; Haufler, R. E.; Chibante, L. P. F.; Fure, J.; Wang, L.; Alford, J. M.; Smalley, R. E. *J. Phys. Chem.* **1991**, *95*, 7564.
(15) Clemmer, D. E.; Hunter, J. M.; Shelomov, K. B.; Jarrold, M. F. *Nature* **1994**, *372*, 248.
(16) Iijima, S.; Ichihashi, T. *Nature* **1993**, *363*, 603.
(17) Nash, B. K.; Rao, B. K.; Jena, P. *J. Chem. Phys.* **1996**, *105*, 11020.
(18) Cao, Z. *J. Mol. Struct. (THEOCHEM)* **1996**, *365*, 211.
(19) Roszak, S.; Balasubramanian, K. *J. Phys. Chem. A* **1997**, *101*, 2666.
(20) Sumathi, R.; Hendrickx, M. *Chem. Phys. Lett.* **1998**, *287*, 496.
(21) Jackson, P.; Gadd, G. E.; Mackey, D. W.; van der Wall, H.; Willett, G. D. *J. Phys. Chem. A* **1998**, *102*, 8941.
(22) Arbuznikov, A. V.; Hendrickx, M.; Vanquickenborne, L. G. *Chem. Phys. Lett.* **1999**, *310*, 515.
(23) Arbuznikov, A. V.; Hendrickx, M. *Chem. Phys. Lett.* **2000**, *320*, 575.
(24) Rey, C.; Alemany, M. M. G.; Dieguez, O.; Gallego, L. J. *Phys. Rev. B* **2000**, *62*, 12640.
(25) Noya, E. G.; Longo, R. C.; Gallego, L. J. *J. Chem. Phys.* **2003**, *119*, 11130.
(26) Majumdar, D.; Roszak, S.; Balasubramanian, K. *J. Chem. Phys.* **2003**, *118*, 130.
(27) Zhai, H. J.; Wang, L. S.; Jena, P.; Gutsev, G. L.; Bauschlicher, C. W., Jr. *J. Chem. Phys.* **2004**, *120*, 8996.
(28) Hendrickx, M. F. A.; Clima, S. *Chem. Phys. Lett.* **2004**, *388*, 284.
(29) Hendrickx, M. F. A.; Clima, S. *Chem. Phys. Lett.* **2004**, *388*, 290.
(30) Ryzhkov, M. V.; Ivanovskii, A. L.; Delley, B. T. *Chem. Phys. Lett.* **2005**, *404*, 400.
(31) Li, X.; Wang, L. S. *J. Chem. Phys.* **1999**, *111*, 8389.
(32) Rayon, V. M.; Redondo, P.; Barrientos, C.; Largo, A. *Chem.—Eur. J.* **2006**, *12*, 6963.
(33) Rayon, V. M.; Redondo, P.; Barrientos, C.; Largo, A. *Chem. Phys. Lett.* **2006**, *422*, 289.
(34) Becke, A. D. *J. Chem. Phys.* **1986**, *84*, 4524.
(35) Becke, A. D. *J. Chem. Phys.* **1988**, *88*, 2547.
(36) Lee, C.; Yang, W.; Parr, R. G. *Phys. Rev. B* **1988**, *37*, 785.
(37) Becke, A. D. *J. Chem. Phys.* **1988**, *88*, 1053.
(38) Pascoli, G.; Lavendy, H. *Int. J. Mass Spectrom.* **1998**, *181*, 11.
(39) Pople, J. A.; Head-Gordon, M.; Raghavachari, K. *J. Chem. Phys.* **1987**, *87*, 5968.
(40) Krishnan, R.; Binkley, J. S.; Seeger, R.; Pople, J. A. *J. Chem. Phys.* **1980**, *72*, 650.
(41) Wachters, A. J. H. *J. Chem. Phys.* **1970**, *52*, 1033.
(42) Hay, P. J. *J. Chem. Phys.* **1977**, *66*, 4377.
(43) Raghavachari, K.; Trucks, G. W. *J. Chem. Phys.* **1989**, *91*, 1062.
(44) Raghavachari, K.; Trucks, G. W.; Pople, J. A.; Head-Gordon, M. *Chem. Phys. Lett.* **1989**, *157*, 479.
(45) Frisch, M. J.; et al. *Gaussian 98*; Gaussian Inc.: Pittsburgh, PA, 1998.
(46) Amos, R. D.; et al. *MOLPRO*, 2002.1.
(47) Bader, R. F. W. *Atoms in Molecules. A Quantum Theory*; Clarendon Press: Oxford, U.K., 1990.
(48) Popelier, P. L. A. *Comput. Phys. Commun.* **1996**, *93*, 212.
(49) Reed, A. E.; Curtiss, L. A.; Weinhold, F. *Chem. Rev.* **1988**, *88*, 899.
(50) Hay, P. J.; Wadt, W. R. *J. Chem. Phys.* **1985**, *82*, 270.

(51) Wadt, W. R.; Hay, P. J. *J. Chem. Phys.* **1985**, *82*, 284.
(52) Hay, P. J.; Wadt, W. R. *J. Chem. Phys.* **1985**, *82*, 299.
(53) NIST Chemistry WebBook, http://webbook.nist.gov/chemistry.
(54) Bader, R. F. W. *Chem. Rev.* **1991**, *91*, 893.
(55) Cremer, D.; Kraka, E. *Angew. Chem., Int. Ed. Engl.* **1984**, *23*, 627.
(56) Largo, A.; Redondo, P.; Barrientos, C. *J. Am. Chem. Soc.* **2004**, *126*, 14611.
(57) Clementi, E.; Kistenmacher, H.; Popkie, H. *J. Chem. Phys.* **1973**, *58*, 2460.
(58) Nielsen, I. M. B.; Allen, W. D.; Csaszar, A. G.; Schaefer, H. F. *J. Chem. Phys.* **1997**, *107*, 1195.
(59) Abrams, M. L.; Sherrill, C. D. *J. Chem. Phys.* **2004**, *121*, 9211.
(60) Sherrill, C. D.; Piecuch, P. *J. Chem. Phys.* **2005**, *122*, 124104.
(61) Lias, S. G. Ionization Energy Evaluation, in *NIST Chemistry WebBook*; NIST Standard Reference Database Number 69; Linstrom, P. J., Mallard, W. G., Eds.; National Institute of Standards and Technology: Gaithersburg, MD, June 2005 (http://webbook.nist.gov).